Prevention of intrahepatic metastasis of liver cancer by suicide gene therapy and chemokine ligand 2/monocyte chemoattractant protein-1 delivery in mice

Title:

Prevention of Intrahepatic Metastasis of Liver Cancer by Suicide Gene Therapy and CCL2/MCP-1 Delivery in Mice

Kaheita Kakinoki [1], Yasunari Nakamoto [1], Takashi Kagaya [1], Tomoya Tsuchiyama [1], Yoshio Sakai [1], Tohru Nakahama [1], Naofumi Mukaida [2], Shuichi Kaneko [1]

[1] Disease Control and Homeostasis, Graduate School of Medical Science,

[2] Division of Molecular Bioregulation, Cancer Research Institute,

Kanazawa University, 13-1 Takara-machi, Kanazawa 920-8641, Japan

Address correspondence to: Shuichi Kaneko, Disease Control and Homeostasis, Graduate School of Medical Science, Kanazawa University, 13-1 Takara-machi, Kanazawa 920-8641, Japan

Phone: +81-76-265-2231

Fax: +81-76-234-4250

E-mail: skaneko@m-kanazawa.jp

Keywords: Monocytes/Macrophages, Chemokines, Hepatocellular Carcinoma

Running title: Prevention of IM by Suicide Gene and CCL2/MCP-1

Abbreviations:

BNL, BNL 1ME A.7R.1; MOI, multiplicity of infection; GCV, ganciclovir; HCC, hepatocellular carcinoma; IM, intrahepatic metastasis; MC, multicentric carcinogenesis; HSV-tk, herpes simplex virus thymidine kinase; $TICD_{50}$, 50% tissue culture infectious dose; GpA, rabbit beta-globin poly (A) site; LacZ, beta-galactosidase; CCL2, chemokine ligand 2; MCP-1, human monocyte chemoattractant protein-1; VEGF, vascular endothelial growth factor; CAG, CAG promoter; rAd, recombinant adenovirus vector; Ad-tk, rAd expressing HSV-tk; Ad-MCP1, rAd expressing CCL2/MCP-1; Ad-LacZ, rAd expressing LacZ; iNOS, inducible nitric oxide synthase; Arg-I, arginase I

Abstract

Background The prognosis of patients with hepatocellular carcinoma (HCC) remains poor, largely due to intrahepatic metastasis (IM). Using a mouse model of IM, we investigated whether monocyte chemoattractant protein-1 (CCL2/MCP-1) could potentiate the antitumor effects of the herpes simplex virus thymidine kinase/ganciclovir (HSV-tk/GCV) system.

Methods Mouse hepatoma cells infected with recombinant adenovirus vectors (rAds) expressing HSV-tk, CCL2/MCP-1, and LacZ at multiplicities of infection (MOIs) of Ad-tk/Ad-MCP1 = 3/0.03 (T/M^{Low}), 3/3 (T/M^{High}), and Ad-tk/Ad-LacZ = 3/3 (T/L) were injected into BALB/c mice.

Results Intrahepatic tumor growth was significantly lower in T/M^{Low} mice. In contrast, no tumor suppression was observed in T/M^{High} mice. The tumor-specific cytolytic activities of splenocytes from T/M^{Low} and T/M^{High} mice were comparable. Immunohistochemical analysis of liver tissues showed similar infiltration by $Mac\text{-}1^{+}$ and T cells in these animals, whereas the proportions of classical activated (M1) monocytes/macrophages were significantly higher in T/M^{Low} mice. In addition, IL-12 production was elevated in these tissues. VEGF-A expression and $CD31^{+}$ microvessels

were increased in T/M^{High} mice.

Conclusions Collectively, these results demonstrate that an adequate amount of CCL2/MCP-1, together with the HSV-tk/GCV system, may induce Th1-polarized antitumor effects without inducing tumor angiogenesis in the microenvironment of intrahepatic HCC progression.

Introduction

Primary liver cancer is the fifth most common neoplasm in the world and the third most common cause of cancer-related deaths [1, 2]. Despite the development of novel modalities for treatment of hepatocellular carcinoma (HCC), including transcatheter arterial embolization, percutaneous ablation, surgical resection and liver transplantation, the prognosis of patients with HCC still remains relatively poor. One of the major factors responsible for these unsatisfactory outcomes is the high frequency of intrahepatic recurrence after curative treatment [1, 2]. Intrahepatic recurrence is due to two mechanisms; intrahepatic metastasis (IM) originating from the primary cancer, and a second primary cancer arising from multicentric carcinogenesis (MC). IM may correlate with early recurrence and poor prognosis, whereas MC is associated with relatively good prognosis [3-5].

To develop novel antitumor strategies for HCC, we have investigated the effectiveness of immune gene therapy using suicide genes and chemokine molecules, including chemokine ligand 2/monocyte chemoattractant protein-1 (CCL2/MCP-1) [6-8]. CCL2/MCP-1 is a chemokine that regulates the recruitment of

monocytes/macrophages to inflammatory sites and tumor tissues as well as their activation, including lysosomal enzyme release and tumoricidal activity, and is functional in both mice and humans [9]. Transfectant-derived CCL2/MCP-1 has been found to successfully recruit monocytes into tumor tissue [10, 11]. We recently described a combination strategy for the treatment of HCC, consisting of the herpes simplex virus thymidine kinase/ganciclovir (HSV-tk/GCV) system and CCL2/MCP-1 gene delivery. We found that adenovirally delivered CCL2/MCP-1 enhanced the antitumor effects of the HSV-tk/GCV system by activating innate immune responses involving monocytes/macrophages, as well as demonstrating prolonged efficacy mediated by NK cells [6-8]. These experiments were performed in athymic nude mice, deficient in acquired immune responses, subcutaneously transplanted with HCC.

In this study, we have used a liver metastasis model, in which tumor cells were infused through the portal vein (PV), to investigate whether CCL2/MCP-1 gene delivery could potentiate the antitumor effects of the suicide gene system. Our results indicate that the antitumor effects of the suicide gene are enhanced by codelivery of an adequate amount of CCL2/MCP-1. These antitumor effects were associated with the recruitment of monocytes/macrophages and T cells, T helper 1 (Th1) cytokine gene expression and the induction of splenocyte cytolytic activity. These findings indicate

that CCL2/MCP-1 has an immunomodulatory effect on suicide gene therapy for HCC by orchestrating the innate and acquired immune responses.

Materials and methods

Animals

Male BALB/cA Jcl mice, 6-8 weeks of age, were obtained from CLEA Japan Inc. (Tokyo, Japan), maintained at constant room temperature (25 °C) and provided with free access to standard diet and tap water throughout, according to institutional guidelines.

Cell lines and cell culture

The mouse HCC cell line BNL 1ME A.7R.1 (BNL) and the mouse colon cancer cell line colon 26 clone 20 (CT 26), derived from BALB/c mice (H-2d), were cultured in Dulbecco's modified Eagle medium (DMEM) supplemented with 10 % heat-inactivated (30 min at 56 °C) fetal bovine serum (FBS), non-essential amino acids, sodium pyruvate, HEPES buffer, 2 mM glutamate, 1 mM penicillin/streptomycin and 0.2 mM gentamicin (Gibco, Long Island, NY) at 37 °C in 5 % CO2.

Recombinant adenovirus vectors

The following replication-defective adenovirus vectors, driven by the CAG promoter [12], were prepared by recombinant DNA technology: Ad-tk, which expresses

the HSV-tk gene; Ad-MCP1, which expresses the human CCL2/MCP-1 gene; and Ad-LacZ, which expresses the LacZ gene [13] (Figure 1A). Each recombinant adenovirus vector was purified and titered according to protocols supplied by the manufacturer (Takara, Ootsu, Japan). Briefly, each gene fragment, i.e. HSV-tk, CCL2/MCP-1 and LacZ, was excised from its respective insert-containing pBluescript vector and inserted into the cosmid pAxCA-wt (Takara, Ootsu, Japan), which contains essentially the full-length adenovirus type 5 genome apart from the E1 and E3 regions, thus generating the pAxCA gene (Figure 1A). The rAds were generated by transfecting 293 cells with pAxCA-gene and adenovirus 5-dIX DNA-terminal protein complex. These rAds were propagated in 293 cells [14], and viral stocks were prepared by standard protocols [15]. The titers of rAds were determined by the 50 % tissue culture infectious dose ($TCID_{50}$) method [16].

ELISA for CCL2/MCP-1

Aliquots of 2.5×10^4 BNL cells were seeded in 3.0 ml of culture media in 6-well tissue culture plate. After 24 hours, the cells were infected with Ad-MCP1 and Ad-MCP1, together with Ad-tk, at various multiplicities of infections (MOIs). After 24 hours, the media were collected from the wells, and the concentrations of CCL2/MCP-1

were determined by ELISA. Briefly, each well of a 96 well microtiter plate (Nalgene, Rochester, NY) was coated with 0.05 M carbonate buffer (pH 9.6) containing monoclonal anti-human CCL2/MCP-1 antibody (ME 6.1; 1 μg/ml) overnight at 4 °C. After washing with phosphate buffered saline (PBS) containing 0.05 % Tween 20 (PBS-T), the plates were blocked with PBS containing 1 % BSA for 1 hour at 37 °C. Diluted culture medium or various concentrations of recombinant CCL2/MCP-1 were added to duplicate wells and incubated for 2 hours at 37 °C. The plates were washed, incubated with rabbit anti-CCL2/MCP-1 antibodies (1 μg/ml) for 2 hours at 37 °C, washed again and incubated with alkaline phosphatase-conjugated goat anti-rabbit antibody (1/12,000; Tago, Burlingame, CA) for 2 hours at 37 °C. The plates were washed, aliquots of 1 mg/ml p-nitrophenylphosphate (Sigma, St. Louis, MO) in 1 M diethanolamine (pH 9.8) supplemented with 0.5 mM $MgCl_2$ were added to the wells, and the plates were incubated for 40 min at room temperature. After addition of 1 M NaCl, the optical density (405 nm wavelength-OD405) was assessed using an ELISA plate reader (MTP-120; Corona Electric, Ibaragi, Japan). All experiments were repeated in triplicate.

Disease Model

To evaluate the direct antitumor effect of CCL2/MCP-1, 1×10^7 BNL cells suspended in 0.5 ml of culture medium were infected *in vitro* with CCL2/MCP-1 at various MOIs: 0.03 (M^{Low}), 0.3 (M^{Mod}), and 3 (M^{High}), Ad-LacZ at an MOI of 3 (L), or PBS (-). The cells were harvested after 30 min incubation at 37 °C. BALB/c mice were anesthetized by intraperitoneal injection with sodium pentobarbital (Somnopentyl, Schering-Plough Animal Health Corporation, Kenilworth, NJ), and laparotomy was performed. Each mouse was injected with 1×10^6 adenovirus-infected BNL cells in a volume of 0.2 ml PBS containing 2 % FBS or 0.2 ml PBS (-) via PV on day 0. The mice were sacrificed on day 21, and their liver tissues were weighed.

To determine whether CCL2/MCP-1 can enhance the antitumor effects of the HSV-tk/GCV system, BNL cells were infected with Ad-tk, Ad-MCP1 and Ad-LacZ at various MOIs: Ad-tk/Ad-MCP1 = 3/0.03 (T/M^{Low}), 3/0.3 (T/M^{Mod}) and 3/3 (T/M^{High}), Ad-tk/Ad-LacZ = 3/3 (T/L), and Ad-LacZ = 6 (N/L). BALB/c mice were anesthetized and each was injected via portal vein with 1×10^6 adenovirus-infected BNL cells on day 0, followed by intraperitoneal injection of 75 mg/kg/day ganciclovir on days 2-6. The mice were sacrificed on day 21, and the livers were removed and weighted. Additionally, in another series of experience, the livers removed from the mice on days 1, 3, 7 and 14 were processed for immunohistochemistry and quantitative real-time PCR.

Simultaneously, their splenocytes were tested for cytolytic activity against ^{51}Cr-labeled BNL cells.

Histopathological and immunohistochemical analysis

Liver sections were fixed in 10 % zinc-buffered formalin and stained with hematoxylin and eosin (H-E). For histological evaluation, mouse livers were harvested, embedded in tissue-Tek® OCT embedding medium (Sakura Finetek, Torrance, CA) and stored at -80 °C until use, except those stained for CD31 (Abcam, Cambridge, MA), arginase I (Arg-I; BD Biosciences, Franklin Lakes, NJ) and inducible nitric oxide synthase (iNOS; Thermo Fisher Scientific, Fremont, CA). Cryostat sections of frozen tissues were fixed in cold acetone for 10 minutes and rinsed three times with PBS. The tissue samples used for CD31, iNOS and Arg-I staining were fixed in 10 % phosphate-buffered formalin and embedded in paraffin. Following blocking of nonspecific tissue avidin and biotin with a blocking kit (Vector Laboratories, Burlingame, CA), the slides were incubated with biotin-conjugated monoclonal antibody against Mac-1 (CD11b), CD4, CD8 (PharMingen, San Jose, CA) or Arg-I or polyclonal antiserum against CD31 or iNOS for 30 minutes at room temperature. Biotin-conjugated rat IgG2b, kappa was used as the negative control. The reaction was

visualized using a Vectastain® ABC Standard Kit (Vector Laboratories, Burlingame, CA), followed by counterstaining with hematoxylin.

Real-time quantitative RT-PCR

The Frozen liver specimens containing necrotic liver tissues or tumor tissues were broken into fine pieces and total RNA was extracted from liver tissues using a ToTALLY RNA® kit (Ambion, Austin, TX) according to the manufacturer's protocol. Total RNA (1 μg) was reverse transcribed into cDNA using a SuperScript® first-strand synthesis system for RT-PCR (Invitrogen, Carlsbad, CA). The first strand cDNA was used for real-time quantitative PCR using the ABI PRISM 7900 (Applied Biosystems, Foster City, CA) with TaqMan® Master Mix (Applied Biosystems), and primers and probes for IL-4, IL-10, IL-12, IL-18, IFNγ, VEGF-A and 18S ribosome (sequences available on request) (Applied Biosystems). Expression of cytokine mRNA in each sample was normalized relative to that of 18S ribosome mRNA.

Cytotoxic T lymphocyte assay (^{51}Cr release assay)

The cytolytic activity of mouse spleen cells was assessed by a ^{51}Cr release assay, as described[17]. Briefly, each treated mouse was sacrificed on day 14, splenocytes

were harvested aseptically and mashed in alpha-MEM medium (Gibco) with 10 % FBS, and suspensions of single spleen cells were prepared. Spleen cells were cultured with mitomycin C (MMC; Sigma, ST. Louis, MO) (400 μg/4 ml, 1 mg/ml in HBSS) treated BNL or CT26 cells in complete alpha-MEM medium containing 10 % FBS and 2.5 % EL-4 culture supernatant (a source of T cell growth factor) for 5 days. Target cells consisted of 3×10^5 BNL cells labeled with 0.3 mCi Na251CrO4 (NEN Life Science Products, Boston, MA) at 37 °C for 1 hour. Effector spleen cells were incubated with 5 $\times 10^3$ target cells in 96-well plates at various effector/target ratios for 4 hours at 37 °C, and the ^{51}Cr released into the culture supernatants was quantified by scintillation counting. Percent specific cytotoxicity was calculated according to the equation: [100 × (experimental release - spontaneous release) / (maximum release - spontaneous release)]. Spontaneous release was defined as the ^{51}Cr in the supernatant of target cells incubated for 4 hours, and maximum release was defined as ^{51}Cr in the supernatant of target cells treated with 2 % Triton-X. Experiments were performed three times and results were expressed as the mean ± SE. Tumor specificity was determined based on differences between BNL and CT 26 cells. All results presented are the means of triplicate assays.

Results

CCL2/MCP-1 production of recombinant adenoviruses in vitro

The production of CCL2/MCP-1 was evaluated by measuring the concentrations in culture media of BNL cells infected with varying MOIs of Ad-MCP1 and Ad-MCP1 plus Ad-tk by ELISA (Figure 1B). The production of CCL2/MCP-1 by cells infected with Ad-MCP1 increased in proportion to the MOI. Importantly, its production by Ad-MCP1 infected cells was not changed when these cells were further infected with Ad-tk (Ad-MCP1 plus Ad-tk), indicating that CCL2/MCP-1 production by Ad-MCP1 was not influenced by coinfection with Ad-tk in BNL cells. In addition, the functional properties of CCL2/MCP-1 produced by this rAd were defined previously [6-8].

Intrahepatic tumor development following transfer of HCC cells infected with recombinant adenoviruses

To evaluate the direct antitumor effect of CCL2/MCP-1 in an immunocompetent mouse model of IM, mice were injected via the PV with BNL cells infected with Ad-MCP1 or Ad-LacZ at various MOIs (Figure 1C). When whole livers were weighed on day 21, the weights of M^{Low} (n=4), M^{Mod} (n=7) and M^{High} (n=6) were

comparable to those of L (n=4) mice, indicating that delivery of CCL2/MCP-1 gene did not promote or suppress the growth of tumor cells in this model.

To determine whether CCL2/MCP-1 gene delivery can potentiate the antitumor effects of the HSV-tk/GCV system, mice were injected with BNL cells infected with rAds (Ad-tk, Ad-MCP1 and Ad-LacZ) at various MOIs as described in **Materials and methods**. Whole livers were weighed on day 21, and the weights of T/M^{Low} (n=14), T/M^{Mod} (n=12), T/M^{High} (n=11) and T/L (n=10) mice were compared to those of N/L (n=10) mice. The reduction in liver weight for the T/L mice was due to HSV-tk/GCV system alone and those for T/M^{Low}, T/M^{Mod} and T/M^{High} were due to the treatment in combination with CCL2/MCP-1. Mean liver weight (± SEM) was significantly lower in T/M^{Low} mice than in T/L mice (3.91 ± 0.36 g vs. 5.80 ± 0.58 g ; $P < 0.01$) (Figure 1D and 1E), due to the reduced growth of implanted tumor cells in the former. In contrast, the increase in liver weight was not suppressed in T/M^{Mod} and T/M^{High} mice whose tumor cells had been treated with higher titers of Ad-MCP1. Thus, only low level CCL2/MCP-1 provided additional antitumor effects and these results indicate that delivery of adequate amounts of Ad-MCP1 enhanced the antitumor effects of the HSV-tk/GCV system against intrahepatic tumor cells.

Serial analysis of liver histology following tumor cell transfer

To monitor the course of tumor development following HCC cell transfer, mouse livers were harvested on days 1, 3, 7 and 14. Livers harvested on day 1 from all groups of mice injected with BNL cells showed multiple white patches on their surfaces. Histologically, hepatocyte degeneration and necrosis were observed in these lesions, suggesting that the reduction of PV flow by transferred tumor cells induced focal ischemic necrosis in the livers (Figure 2, closed arrowheads). Although the extent of necrosis was similar among all groups, inflammatory cell infiltration in the area of necrosis was greater in T/M^{Low}, T/M^{High} and T/L than in N/L mice. On day 3, cellular infiltration disappeared, and tumor cell growth was observed in areas surrounding the necrotic regions. On day 7, proliferation of viable tumor cells surrounding the necrosis was seen in the livers of N/L mice, with the necrotic tissues completely replaced by tumor cells. Tumor growth was moderately inhibited in T/L mice and greatly inhibited in T/M^{Low} mice. There was no difference between T/L and T/M^{High} mice (not shown). On day 14, the necrotic areas were almost absorbed in all mice. In N/L mice, the tumor cells grew progressively and the tumor masses became larger. Tumor volume was relatively lower in T/L than in N/L mice, but there was no significant difference between T/L and T/M^{High} mice. The greatest degree of tumor growth inhibition was

observed in T/M^{Low} mice (Figure 2).

Recruitment of immune cells in liver

To evaluate the involvement of immune responses in the CCL2/MCP-1 associated enhancement of the antitumor effects of rAd expressing HSV-tk, we assessed the recruitment of Mac-1^+ monocytes/macrophages and $CD4^+$ and $CD8^+$ T lymphocytes immunohistochemically (Figure 3).

T/M^{Low} and T/M^{High} mouse liver tissues harvested on day 1 showed marked infiltration of Mac-1^+ cells in the necrotic areas induced by tumor cell injection (Figure 3A). Quantitative morphometric analysis showed that the numbers of Mac-1^+ cells were significantly higher in liver tissues of T/M^{Low} and T/M^{High} mice [mean ± SEM of 40 high power (× 400) fields of necrotic liver tissues: 46.5 ± 3.7 and 46.9 ± 3.7; $P < 0.05$ and $P < 0.01$, respectively] compared with T/L mice [35.2 ± 2.4]. Macrophages can be activated not only by CCL2/MCP-1, but also by tumor cells treated with Ad-tk [6]. In T/L mice, these cells may induce moderate infiltration of Mac-1^+ cells (Figure 3B). These findings indicate that the codelivery of the HSV-tk and CCL2/MCP-1 genes was associated with a higher degree of infiltration of Mac-1^+ monocytes/macrophages during the initial period of tumor development. Additionally, to investigate whether the

recruited monocytes/macrophages were polarized towards the M1 or M2 phenotype, we performed immunohistochemical analysis using antibodies against iNOS (M1) and Arg-I (M2) [17, 18] (Figure 3C). The proportion of $iNOS^+$ (M1 subset) cells among the inflammatory cells was significantly higher in T/M^{Low} than in T/M^{High} mice [mean numbers ± SEM (per 100 inflammatory cells) of eight high power (× 400) fields of necrotic liver tissues: 23.0 ± 2.7 and 10.8 ± 2.5; $P < 0.01$, respectively]. Arg-I^+ (M2 subset) cells were not specifically detected, probably due to large amounts of the enzyme present in liver tissues.

Similarly, liver tissues obtained on day 14 after HCC cell transfer were immunohistochemically analyzed for immune cell infiltration. In both T/M^{Low} and T/M^{high} mice, the tumor foci were heavily infiltrated by $CD4^+$ and $CD8^+$ T cells (Figure 3D). Quantitative morphometric analysis showed that the numbers of $CD4^+$ and $CD8^+$ T cells were higher in T/M^{Low} [mean numbers ± SEM (per 100 tumor cells) of eight high power (× 400) fields of liver tissues: 11.1 ± 2.5 and 8.1 ± 2.7; $P < 0.05$ and $P < 0.05$, respectively] and T/M^{High} [7.1 ± 1.9 and 7.1 ± 0.7; N.S and $P < 0.01$, respectively] mice than in T/L mice [4.8 ± 1.1 and 0.3 ± 0.3, respectively] (Figure 3E). These results suggest that the antitumor activities in T/M^{Low} mice may be mediated not only by the activation of macrophages during the initial period of tumor development but also by

the induction of T cell-mediated immune responses during later periods.

Cytokine gene expression in liver

Mice injected with adenovirus-infected HCC cells were sacrificed on day 1 and their liver tissues were analyzed by quantitative real-time RT-PCR for expression of mRNA encoding the cytokines IL-4, IL-10, IL-12, IL-18 and IFN-γ. IL-12 mRNA expression was induced to a greater extent in T/M^{Low} mice than in the other groups ($P < 0.05$). IL-18 mRNA expression tended to be high in the mice treated with CCL2/MCP-1, but these differences were not statistically significant (Figure 4). In contrast, IL-4, IL-10 and IFN-γ mRNA was not detected in any samples. These data suggest that infiltrating monocytes/macrophages induced by CCL2/MCP-1 may be activated to enhance the Th1-polarized responses that contribute to tumor immunity.

Microvessels in HCC

CCL2/MCP-1 has been shown to be associated with angiogenesis [19, 20]. To understand the basis of the different antitumor effects observed in T/M^{Low} and T/M^{High} mice, we immunohistochemically stained microvessels within HCCs for CD31. We found that $CD31^{+}$ microvessels were markedly increased in 7-day tumor tissues of

T/M^{High} mice relative to T/M^{Low} and T/L mice (Figure 5A). These results suggest that angiogenesis induced by large amounts of CCL2/MCP-1 may contribute to tumor growth in T/M^{High} mice.

VEGF gene expression in liver

Liver samples harvested on day 3 were analyzed for expression of VEGF-A mRNA, which encodes an angiogenic factor that may promote tumor growth. Quantitative real-time RT-PCR showed that VEGF-A gene expression was induced to a greater extent in T/M^{High} mice (Figure 5B), suggesting that the CCL2/MCP-1 enhancement of antitumor effects may be offset by VEGF-induced angiogenesis.

Cytotoxic activities of splenocytes

To assess the cytotoxic activities of immune cells derived from mice injected with adenovirus-infected tumor cells, isolated and pulsed splenocytes were incubated with ^{51}Cr-labeled BNL cells in a standard 4-hour cytotoxicity assay (Figure 6). Induction of cytotoxic T lymphocytes (CTLs) specific for BNL cells was higher in T/M^{Low} and T/M^{High} mice than in T/L (N.S.) and N/L ($P < 0.01$) mice, and there was no significance difference between T/M^{Low} and T/M^{High} mice. Since the immunogenicity of

viral vectors or transgene products is known to induce the unfavorable host immune responses, the detection of antitumor CTL activities may be influenced by the responses against rAd vector and HSV-tk [21-23]. Especially, CTL responses against HSV-tk seem to be induced in T/L, T/M^{Low} and T/M^{High} mice. Collectively, the data suggest that cytotoxic activity of CTLs may be enhanced by codelivery of a suicide gene and CCL2/MCP-1, consistent with their in vivo enhancement of antitumor effects.

Discussion

We have shown here that combination gene therapy, using the HSV-tk/GCV system and CCL2/MCP-1 gene delivery, was effective for the treatment of HCC in a mouse model of IM. Delivery of an adequate amount of CCL2/MCP-1 enhanced the antitumor effects of the HSV-tk/GCV system against intrahepatic tumor cells. Necrotic areas induced by HCC tumor cell injection showed marked infiltration of $iNOS^+$ monocytes/macrophages and IL-12 production on day 1, and the tumor foci showed heavy infiltration by $CD4^+$ and $CD8^+$ T cells on day 14. CTLs specific for BNL cells were induced in mice treated with CCL2/MCP-1. In contrast, expression of the angiogenic factor VEGF-A was significantly increased in mice treated with a large amount of CCL2/MCP-1. Collectively, these results suggest that delivery of an adequate amount of CCL2/MCP-1, in conjunction with the HSV-tk/GCV system, may display beneficial antitumor effects, preventing the intrahepatic metastasis of HCC cells.

In the development of this model, we injected 1×10^6 of tumor cells infected with recombinant adenoviruses into the portal vein because the injection of fewer cells, e.g. 10^5, resulted in much diminished frequencies of metastasis in the mice. The injection of large numbers of cells, however, may have caused the embolization of cell

aggregates in the portal vein, which may have contributed to the induction of ischemic necrosis in the liver tissues. The resultant ischemic death of liver cells may be recognized by immune cells including macrophages and may result in macrophage activation and the local release of cytokines and chemokines. However, when the mice were injected with control tumor cells (N/L), we observed little infiltration of immune cells, including macrophages and CD4+ and CD8+ T cells, and these mice developed the largest amounts of tumor tissues. These results indicate that any unfavorable effects due to ischemic cell death were minimal for the development of intrahepatic metastasis in this model.

This model would be more relevant if ganciclovir treatment was delayed, to allow establishment of tumors. Therefore, we performed the additional experiments with ganciclovir treatment at delayed time point, day 3. While there was a trend for small amount of MCP-1 to enhance the antitumor effects of the HSV-tk/GCV system as seen in the experiments on day 1, these differences did not reach statistical significance; T/M^{Low}: 7.64 ± 1.25 (n = 10), T/M^{Mod}: 9.24 ± 0.77 (n = 5), T/M^{High}: 9.65 ± 1.06 (n = 8), T/L: 10.51 ± 1.79 (n = 7) and N/L: 13.94 ± 1.16 (n = 5). Consequently, the experiment in which ganciclovir was added 3 days after tumor inoculation failed to show a significant antitumor effect. The weakness of this work may be still the low relevance of

the tumor model. The reason is that MCP-1 gene expression by rAds may not be enough to enhance antitumor effect at day 3 because the transgene expression gradually diminished with the tumor growth. In our previous studies, MCP-1 production reached peak level on day 2 and decreased after day 3 [6].

Mice treated with small amounts of CCL2/MCP-1 showed enhancement of antitumor effects. The amount of CCL2/MCP-1 delivered, however, was not correlated with monocyte/macrophage accumulation. Although activated monocytes/macrophages are indicative of the potential to eliminate tumor cells [24-26], infiltrating macrophages may enhance tumor growth by secreting growth and angiogenic factors, including VEGF [26-28]. Immunohistochemical analysis of CD31 revealed that microvessels in HCCs were increased in the mice treated with large amounts of CCL2/MCP-1. We also observed a close correlation between the amounts of CCL2/MCP-1 delivered and the levels of VEGF expression. These findings suggest that large amounts of CCL2/MCP-1 may recruit macrophages to induce tumor cell killing and simultaneously to facilitate tumor growth, probably by promoting angiogenesis, thus resulting in a reduction of antitumor effects.

CCL2/MCP-1 is a member of the CC chemokine superfamily that promotes the

migration of macrophages/monocytes, T lymphocytes, natural killer cells and natural killer T cells, not only to sites of inflammation but also to tumor tissues, which may contribute to the inhibition of tumor growth [29-31]. In addition, the production of CCL2/MCP-1 by tumor tissues has been reported to be associated with favorable prognoses in human pancreatic cancer [31] and neuroblastoma [30]. In contrast, CCL2/MCP-1 may promote tumor growth by chemoattracting tumor-associated macrophages for tumor angiogenesis, or by acting on tumor cells as an autocrine growth factor[29, 32, 33]. Consistent with this notion, a Japanese study of 135 breast cancer patients found that the women with high levels of tumor-associated CCL2/MCP-1 showed a significantly shorter relapse-free survival [34]. Taken together, the biological and immunological effects of CCL2/MCP-1 seem to vary greatly depending on the diverse microenvironments of cancer tissues.

Two major types of activated macrophages have been described, M1 (classical) and M2 (alternative) [35-38]. M1 macrophages, which play a critical role in the development of antitumor immunity, are characterized by high IL-12 and low IL-10 production. In contrast, M2 macrophages produce reduced amounts of IL-12 but higher levels of IL-10. We found that IL-12 expression was significantly increased in mice treated with a small amount of CCL2/MCP-1 but not in mice treated with a large

amount of CCL2/MCP-1, despite the marked infiltration of monocytes/macrophages in the latter. In addition, members of the MCP family have been reported to dose-dependently inhibit IL-12 production by antigen-presenting cells (APCs) [39, 40]. Because of the different local concentrations of CCL/MCP-1, we hypothesized that the M1/M2 ratio of recruited monocytes/macrophages may differ in T/MLow and T/MHigh mice. Indeed, we found that the proportions of M1 cells among infiltrating cells were significantly higher in T/M^{Low} than in T/M^{High} mice. Therefore, M1 monocyte/macrophage polarization may be suppressed in mice treated with large amounts of CCL2/MCP-1, resulting in the reduction of antitumor immunity and the promotion of tumor growth.

Significant tumor infiltration of $CD4^+$ and $CD8^+$ T cells 14 days after transfer was observed in mice treated with the HSV-tk/GCV system plus CCL2/MCP-1. Local secretion of CCL2/MCP-1 by tumor cells may lead to the recruitment and activation of antigen-presenting monocytes/macrophages [41, 42]. Once attracted to the tumor tissues, these APCs may ingest pathogenic antigens and transport them to local lymphoid organs, where the antigens are presented to naive T cells, thus establishing a T cell-mediated antitumor response [43]. Tumor growth may thus be impeded by tumor antigen-specific $CD4^+$ and $CD8^+$ T cells.

Although the data presented here appear promising, several problems remain to be solved before clinical application. Our liver metastasis model using a mouse HCC cell line may not be comparable to intrahepatic metastasis of HCC in human patients. However, HCC patients treated by nonsurgical procedures, including percutaneous radiofrequency ablation therapy and transcatheter arterial chemotherapy [44, 45], could also be administered rAds to reduce the incidence of intrahepatic recurrence and metastasis. Our study demonstrated that, in a mouse model, there is a negative impact on tumor development in the presence of a low level of CCL2/MCP-1 whereas high levels of the protein complicate the situation by having a positive impact on tumor growth, i.e. a balance is required. The therapeutic effects may vary with different tumors.

The direct correlation between overexpression of VEGF in tumor cells and tumor angiogenesis has been demonstrated [46], and large amount of CCL2/MCP-1 might be less effective in the treatment of hypervascular tumors such as HCC. However, other cancers resistant to anti-angiogenic drug, e.g. pancreatic cancer [47, 48], probably don’t need a good blood supply for tumor growth. In treatment of hypovascular tumors which are resistant to anti-angiogenic drug, CCL2/MCP-1 may enhance the antitumor effects via activation of M1 macrophages.

Additionally, in the current study we did not perform in vivo delivery

experiments of the vectors to existing tumors. There would be many complicated factors to affect the delivery of HSV-tk and CCL2/MCP-1 genes in therapeutic approaches [49, 50]. Intra-arterial administration of rAds may result in the induction of immunogenicity or cytotoxicity, especially when spread via blood flow. Extremely high-dose rAds have been found to cause severe unexpected side effects [51]. To overcome these problems, highly tumor-specific promoters may be needed. In our previous studies, human alpha-fetoprotein (AFP) promoters specific for liver cancer cells were used in an immunodeficient nude mouse models [6, 52]. A reporter gene was specifically expressed in AFP producing tumors which were xenografted subcutaneously and disseminated in the liver and lung. However, HSV-tk gene expression was not enhanced enough to kill established tumor cells [53] because the transcriptional activity of AFP promoter was relatively low. Furthermore, neither promoters nor delivery systems were found to be specific for the BNL mouse tumor cell line. Although better methods of tumor-specific gene delivery and expression are needed, the use of ex vivo infection techniques has been found to reproduce tumor specific gene expression in vivo.

Conclusions

Although problems with rAds remain to be resolved prior to clinical application, our results suggest that a new strategy, consisting of immune gene therapy accompanied by a suicide gene system, can be used to treat HCC and tumors of other lineages.

Acknowledgments

We thank Akemi Nakano, Yuzu Hasebe and Yui Fujita for assistance with histopathological analysis and immunohistochemistry. We are also grateful to Maki Kawamura and Chiharu Minami for animal care.

References

1. Llovet JM, Burroughs A, Bruix J. Hepatocellular carcinoma. Lancet 2003;362(9399):1907-17.
2. Izumi N, Asahina Y, Noguchi O, et al. Risk factors for distant recurrence of hepatocellular carcinoma in the liver after complete coagulation by microwave or radiofrequency ablation. Cancer 2001;91(5):949-56.
3. Poon RT, Fan ST, Ng IO, Lo CM, Liu CL, Wong J. Different risk factors and prognosis for early and late intrahepatic recurrence after resection of hepatocellular carcinoma. Cancer 2000;89(3):500-7.
4. Arii S, Monden K, Niwano M, et al. Results of surgical treatment for recurrent hepatocellular carcinoma; comparison of outcome among patients with multicentric carcinogenesis, intrahepatic metastasis, and extrahepatic recurrence. J Hepatobiliary Pancreat Surg 1998;5(1):86-92.
5. Miyata R, Tanimoto A, Wakabayashi G, et al. Accuracy of preoperative prediction of microinvasion of portal vein in hepatocellular carcinoma using superparamagnetic iron oxide-enhanced magnetic resonance imaging and computed tomography during hepatic angiography. Journal of gastroenterology

2006;41(10):987-95.

6. Sakai Y, Kaneko S, Nakamoto Y, Kagaya T, Mukaida N, Kobayashi K. Enhanced anti-tumor effects of herpes simplex virus thymidine kinase/ganciclovir system by codelivering monocyte chemoattractant protein-1 in hepatocellular carcinoma. Cancer Gene Ther 2001;8(10):695-704.
7. Tsuchiyama T, Kaneko S, Nakamoto Y, et al. Enhanced antitumor effects of a bicistronic adenovirus vector expressing both herpes simplex virus thymidine kinase and monocyte chemoattractant protein-1 against hepatocellular carcinoma. Cancer Gene Ther 2003;10(4):260-9.
8. Tsuchiyama T, Nakamoto Y, Sakai Y, et al. Prolonged, NK cell-mediated antitumor effects of suicide gene therapy combined with monocyte chemoattractant protein-1 against hepatocellular carcinoma. J Immunol 2007;178(1):574-83.
9. Rollins BJ, Sunday ME. Suppression of tumor formation in vivo by expression of the JE gene in malignant cells. Mol Cell Biol 1991;11(6):3125-31.
10. Hirose K, Hakozaki M, Nyunoya Y, et al. Chemokine gene transfection into tumour cells reduced tumorigenicity in nude mice in association with neutrophilic infiltration. Br J Cancer 1995;72(3):708-14.
11. Huang S, Singh RK, Xie K, et al. Expression of the JE/MCP-1 gene suppresses

metastatic potential in murine colon carcinoma cells. Cancer Immunol Immunother 1994;39(4):231-8.

12. Kanegae Y, Lee G, Sato Y, et al. Efficient gene activation in mammalian cells by using recombinant adenovirus expressing site-specific Cre recombinase. Nucleic Acids Res 1995;23(19):3816-21.
13. Miyake S, Makimura M, Kanegae Y, et al. Efficient generation of recombinant adenoviruses using adenovirus DNA-terminal protein complex and a cosmid bearing the full-length virus genome. Proc Natl Acad Sci U S A 1996;93(3):1320-4.
14. Sato Y, Tanaka K, Lee G, et al. Enhanced and specific gene expression via tissue-specific production of Cre recombinase using adenovirus vector. Biochemical and biophysical research communications 1998;244(2):455-62.
15. Matthews DA, Russell WC. Adenovirus protein-protein interactions: hexon and protein VI. The Journal of general virology 1994;75 (Pt 12):3365-74.
16. Kanegae Y, Makimura M, Saito I. A simple and efficient method for purification of infectious recombinant adenovirus. Jpn J Med Sci Biol 1994;47(3):157-66.
17. Benoit M, Desnues B, Mege JL. Macrophage polarization in bacterial infections. J Immunol 2008;181(6):3733-9.
18. Redente EF, Orlicky DJ, Bouchard RJ, Malkinson AM. Tumor signaling to the bone

marrow changes the phenotype of monocytes and pulmonary macrophages during urethane-induced primary lung tumorigenesis in A/J mice. The American journal of pathology 2007;170(2):693-708.

19. Salcedo R, Ponce ML, Young HA, et al. Human endothelial cells express CCR2 and respond to MCP-1: direct role of MCP-1 in angiogenesis and tumor progression. Blood 2000;96(1):34-40.

20. Koga M, Kai H, Egami K, et al. Mutant MCP-1 therapy inhibits tumor angiogenesis and growth of malignant melanoma in mice. Biochemical and biophysical research communications 2008;365(2):279-84.

21. Berger C, Flowers ME, Warren EH, Riddell SR. Analysis of transgene-specific immune responses that limit the in vivo persistence of adoptively transferred HSV-TK-modified donor T cells after allogeneic hematopoietic cell transplantation. Blood 2006;107(6):2294-302.

22. Raty JK, Lesch HP, Wirth T, Yla-Herttuala S. Improving safety of gene therapy. Current drug safety 2008;3(1):46-53.

23. Schagen FH, Ossevoort M, Toes RE, Hoeben RC. Immune responses against adenoviral vectors and their transgene products: a review of strategies for evasion. Critical reviews in oncology/hematology 2004;50(1):51-70.

24. Bonta IL, Ben-Efraim S. Involvement of inflammatory mediators in macrophage antitumor activity. J Leukoc Biol 1993;54(6):613-26.

25. Hock H, Dorsch M, Kunzendorf U, Qin Z, Diamantstein T, Blankenstein T. Mechanisms of rejection induced by tumor cell-targeted gene transfer of interleukin 2, interleukin 4, interleukin 7, tumor necrosis factor, or interferon gamma. Proc Natl Acad Sci U S A 1993;90(7):2774-8.

26. Mantovani A, Bottazzi B, Colotta F, Sozzani S, Ruco L. The origin and function of tumor-associated macrophages. Immunol Today 1992;13(7):265-70.

27. Leung SY, Wong MP, Chung LP, Chan AS, Yuen ST. Monocyte chemoattractant protein-1 expression and macrophage infiltration in gliomas. Acta Neuropathol (Berl) 1997;93(5):518-27.

28. Sunderkotter C, Steinbrink K, Goebeler M, Bhardwaj R, Sorg C. Macrophages and angiogenesis. J Leukoc Biol 1994;55(3):410-22.

29. Conti I, Rollins BJ. CCL2 (monocyte chemoattractant protein-1) and cancer. Seminars in cancer biology 2004;14(3):149-54.

30. Raffaghello L, Cocco C, Corrias MV, Airoldi I, Pistoia V. Chemokines in neuroectodermal tumour progression and metastasis. Seminars in cancer biology 2009;19(2):97-102.

31. Monti P, Leone BE, Marchesi F, et al. The CC chemokine MCP-1/CCL2 in pancreatic cancer progression: regulation of expression and potential mechanisms of antimalignant activity. Cancer research 2003;63(21):7451-61.

32. Loberg RD, Ying C, Craig M, Yan L, Snyder LA, Pienta KJ. CCL2 as an important mediator of prostate cancer growth in vivo through the regulation of macrophage infiltration. Neoplasia (New York, NY 2007;9(7):556-62.

33. Porta C, Subhra Kumar B, Larghi P, Rubino L, Mancino A, Sica A. Tumor promotion by tumor-associated macrophages. Advances in experimental medicine and biology 2007;604:67-86.

34. Ueno T, Toi M, Saji H, et al. Significance of macrophage chemoattractant protein-1 in macrophage recruitment, angiogenesis, and survival in human breast cancer. Clin Cancer Res 2000;6(8):3282-9.

35. Mosser DM. The many faces of macrophage activation. J Leukoc Biol 2003;73(2):209-12.

36. Edwards JP, Zhang X, Frauwirth KA, Mosser DM. Biochemical and functional characterization of three activated macrophage populations. J Leukoc Biol 2006.

37. Mantovani A, Sica A, Sozzani S, Allavena P, Vecchi A, Locati M. The chemokine system in diverse forms of macrophage activation and polarization. Trends

Immunol 2004;25(12):677-86.

38. Gratchev A, Kzhyshkowska J, Kothe K, et al. Mphi1 and Mphi2 can be re-polarized by Th2 or Th1 cytokines, respectively, and respond to exogenous danger signals. Immunobiology 2006;211(6-8):473-86.

39. Braun MC, Lahey E, Kelsall BL. Selective suppression of IL-12 production by chemoattractants. J Immunol 2000;164(6):3009-17.

40. Matsunaga K, Klein TW, Newton C, Friedman H, Yamamoto Y. Legionella pneumophila suppresses interleukin-12 production by macrophages. Infect Immun 2001;69(3):1929-33.

41. Gu L, Tseng S, Horner RM, Tam C, Loda M, Rollins BJ. Control of TH2 polarization by the chemokine monocyte chemoattractant protein-1. Nature 2000;404(6776):407-11.

42. Carr MW, Roth SJ, Luther E, Rose SS, Springer TA. Monocyte chemoattractant protein 1 acts as a T-lymphocyte chemoattractant. Proc Natl Acad Sci U S A 1994;91(9):3652-6.

43. Baggiolini M, Dewald B, Moser B. Human chemokines: an update. Annu Rev Immunol 1997;15:675-705.

44. Curley SA. Radiofrequency ablation of malignant liver tumors. Ann Surg Oncol

2003;10(4):338-47.

45. Tung-Ping Poon R, Fan ST, Wong J. Risk factors, prevention, and management of postoperative recurrence after resection of hepatocellular carcinoma. Ann Surg 2000;232(1):10-24.

46. Mise M, Arii S, Higashituji H, et al. Clinical significance of vascular endothelial growth factor and basic fibroblast growth factor gene expression in liver tumor. Hepatology (Baltimore, Md 1996;23(3):455-64.

47. Kindler HL, Niedzwiecki D, Hollis D, et al. Gemcitabine plus bevacizumab compared with gemcitabine plus placebo in patients with advanced pancreatic cancer: phase III trial of the Cancer and Leukemia Group B (CALGB 80303). J Clin Oncol;28(22):3617-22.

48. Philip PA, Benedetti J, Corless CL, et al. Phase III study comparing gemcitabine plus cetuximab versus gemcitabine in patients with advanced pancreatic adenocarcinoma: Southwest Oncology Group-directed intergroup trial S0205. J Clin Oncol;28(22):3605-10.

49. Cassidy J, Schatzlein AG. Tumour-targeted drug and gene delivery: principles and concepts. Expert reviews in molecular medicine 2004;6(19):1-17.

50. Yu P, Wang X, Fu YX. Enhanced local delivery with reduced systemic toxicity:

delivery, delivery, and delivery. Gene therapy 2006;13(15):1131-2.

51. Marshall E. Gene therapy death prompts review of adenovirus vector. Science 1999;286(5448):2244-5.

52. Kaneko S, Hallenbeck P, Kotani T, et al. Adenovirus-mediated gene therapy of hepatocellular carcinoma using cancer-specific gene expression. Cancer research 1995;55(22):5283-7.

53. Sakai Y, Kaneko S, Sato Y, et al. Gene therapy for hepatocellular carcinoma using two recombinant adenovirus vectors with alpha-fetoprotein promoter and Cre/lox P system. Journal of virological methods 2001;92(1):5-17.

FIGURE LEGENDS

Figure 1. Chemokine ligand 2/monocyte chemoattractant protein-1 (CCL2/MCP-1) production and antitumor effects of recombinant adenovirus vectors (rAds). A; Schematic representation of rAds expressing each gene under the control of a CAG promoter. (a) Ad-MCP1 expressing CCL2/MCP-1, (b) Ad-tk expressing HSV-tk, (c) Ad-LacZ expressing beta-galactosidase gene (LacZ). Solid lines indicate the rAd genome, and the open triangle below each rAd genome represents deletions of adenovirus early regions. The arrow shows the orientation of transcription. GpA, rabbit beta-globin (A) site; CAG, CAG promoter. B; Production of CCL2/MCP-1 by BNL cells infected with rAds at various multiplicity of infections (MOIs). The CCL2/MCP-1 concentrations in culture supernatants were determined by ELISA. Data shown are the means of three independent results with standard error bars. C; Liver weight following transfer of BNL cells infected with Ad-MCP1, Ad-LacZ or PBS (-). Each mouse was injected via the portal vein (PV) with 1×10^6 BNL cells infected with Ad-MCP1 at various MOIs: 0.03 (M^{Low}), 0.3 (M^{Mod}), and 3 (M^{High}), and Ad-LacZ at the MOI of 3 (L), and the whole livers were weighed on day 21. D; CCL2/MCP-1 enhancement of the antitumor effects of the HSV-tk/GCV system against intrahepatic cancer cells. Each

mouse was injected via portal vein with BNL cells (1×10^6) infected with Ad-tk, Ad-MCP1 and Ad-LacZ at various MOIs, Ad-tk/Ad-MCP1 = 3/0.03 (T/M^{Low}), 3/0.3 (T/M^{Mod}) and 3/3 (T/M^{High}), Ad-tk/Ad-LacZ = 3/3 (T/L), and Ad-LacZ = 6 (N/L), and the whole livers were weighed on day 21. E; The macroscopic views of hepatic tumors (open arrowheads) in mice. Tumor growth was markedly suppressed in T/M^{Low} mice. The bars equal 10 mm.

Figure 2. Serial analysis of liver histology following tumor cell transfer. Mouse liver tissues were harvested on days 1, 3, 7 and 14, and stained with hematoxylin and eosin (H-E). On day 1, all mice injected with BNL cells showed multiple white patches on the liver surface (not shown). Histologically, hepatocyte degeneration and necrosis were observed in these lesions, suggesting that the reduction of PV flow by transferred tumor cells induced focal ischemic necrosis in the livers. The area of necrosis significantly infiltrated with inflammatory cells (closed arrowheads) was higher in T/M^{Low}, T/M^{High} and T/L mice than in N/L mice. On day 3, cellular infiltration disappeared and tumor cell growth (closed arrows) was detected in areas surrounding the necrotic regions. On day 7, tumor tissue enlarged and replaced the necrotic areas (open arrows). On day 14, the necrotic areas disappeared and tumor nodules eventually formed (open arrowheads).

Original magnifications × 40 and × 200.

Figure 3. Immunohistochemical evaluation of monocyte/macrophage (A-C) and T cell (D and E) recruitment into liver tissues. A; Monocyte/macrophage detection using anti-Mac-1 monoclonal antibody. Original magnification × 400. B; Quantitative morphometric analysis of Mac-1^+ cells. C; Immunohistochemical evaluation of the polarization towards M1 phenotype of recruited monocytes/macrophages using antibody against inducible nitric oxide synthase (iNOS) (closed arrowheads). D; $CD4^+$ (closed arrows) and $CD8^+$ (open arrows) T cell detection. Original magnification × 400. E; Quantitative morphometric analysis of $CD4^+$ and $CD8^+$ T cells.

Figure 4. Real-time quantitative RT-PCR for IL-12 and IL-18 mRNA expressions in liver on day 1. IL-12 gene expression was significantly higher in T/M^{Low} mice than in the other groups ($P < 0.05$).

Figure 5. Evaluation of tumor angiogenesis. A; Morphometric analysis of microvessels in tumor tissues using H-E staining and CD31 immunohistochemical analysis. (a) Representative H-E stained histological sections of day-7 tumor tissues showing

intratumoral microvessels containing red blood cells (closed arrow); endothelial cells were not identified. (b) Representative CD31 immunohistochemical staining showing endothelial cell proliferation in tumor tissues (open arrow). Original magnification × 400. B; Real-time quantitative RT-PCR for VEGF-A mRNA expression in liver on day 3.

Figure 6. Cytotoxic activities of splenocytes. Splenocytes harvested on day 14 from individual mice stimulated with MMC-treated BNL cells for 7 days were tested in a standard 4h cytotoxicity assay with 51Cr-labeled target (BNL) or control (CT26) cells. *$P < 0.05$, **$P < 0.01$, compared with N/L mice.

Fig 1

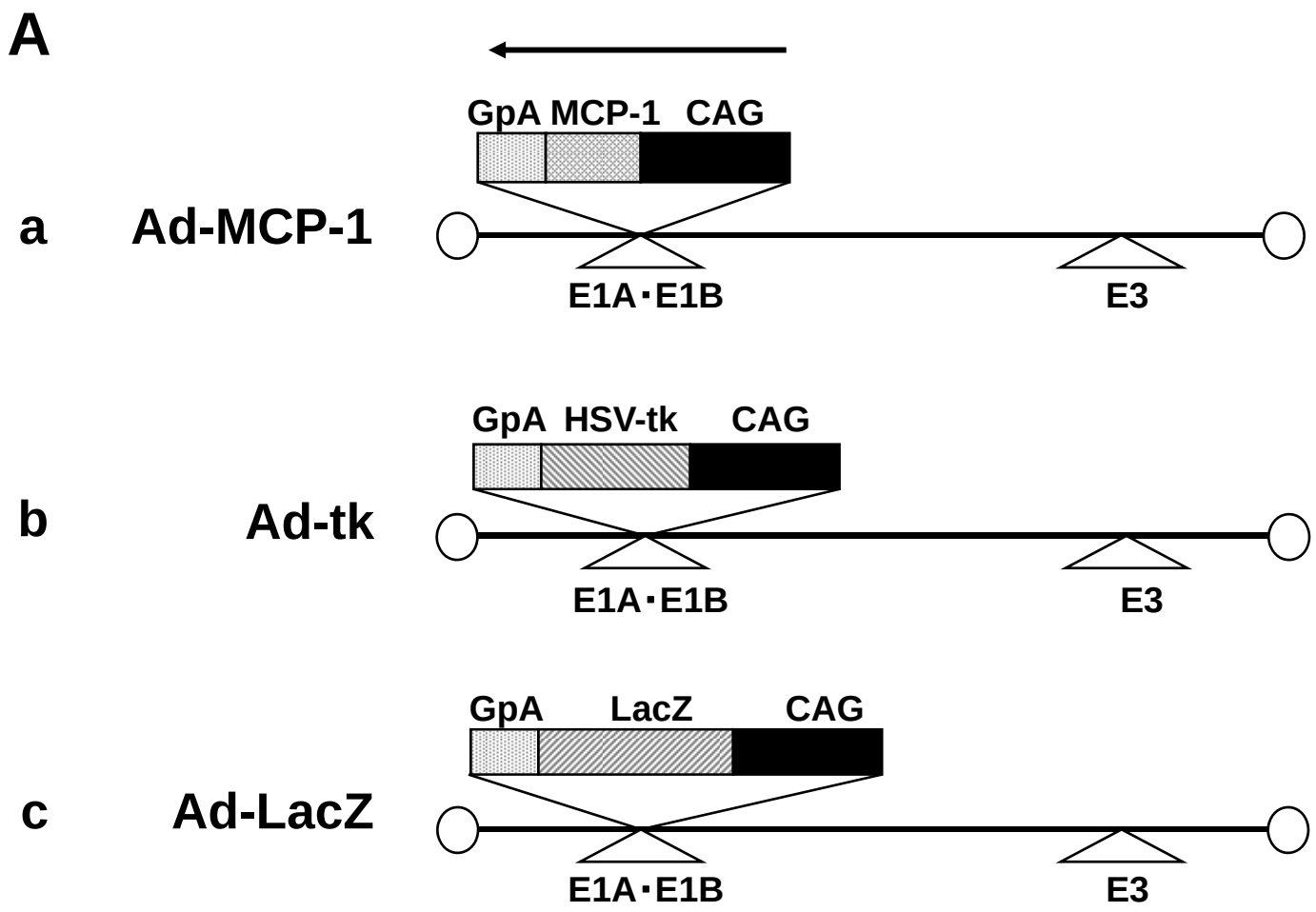
A
a
Ad-MCP-1
GpA MCP-1 CAG
E1A・E1B
E3
b
Ad-tk
GpA HSV-tk CAG
E1A・E1B
E3
c
Ad-LacZ
GpA LacZ CAG
E1A・E1B
E3

Fig 1

B

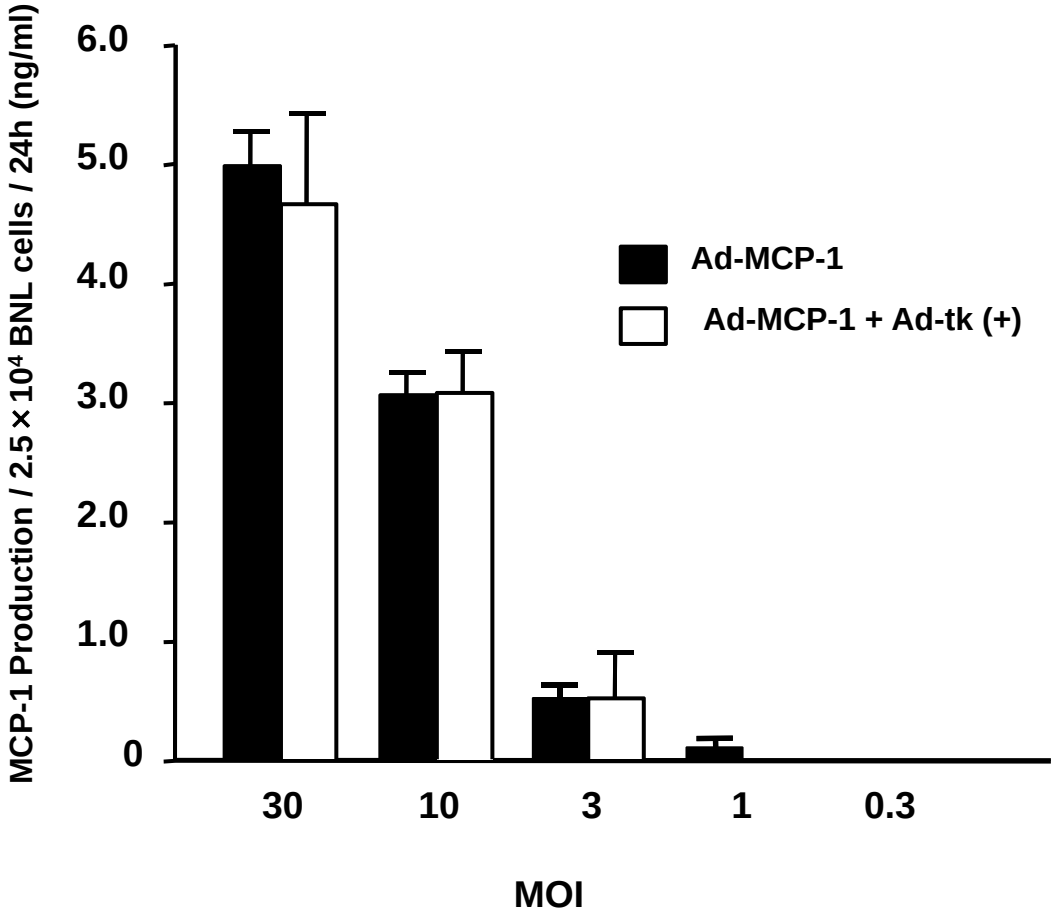
MCP-1 Production / 2.5 × 10⁴ BNL cells / 24h (ng/ml)
6.0
5.0
4.0
3.0
2.0
1.0
0
Ad-MCP-1
Ad-MCP-1 + Ad-tk (+)
30
10
3
1
0.3
MOI

Fig 1

C

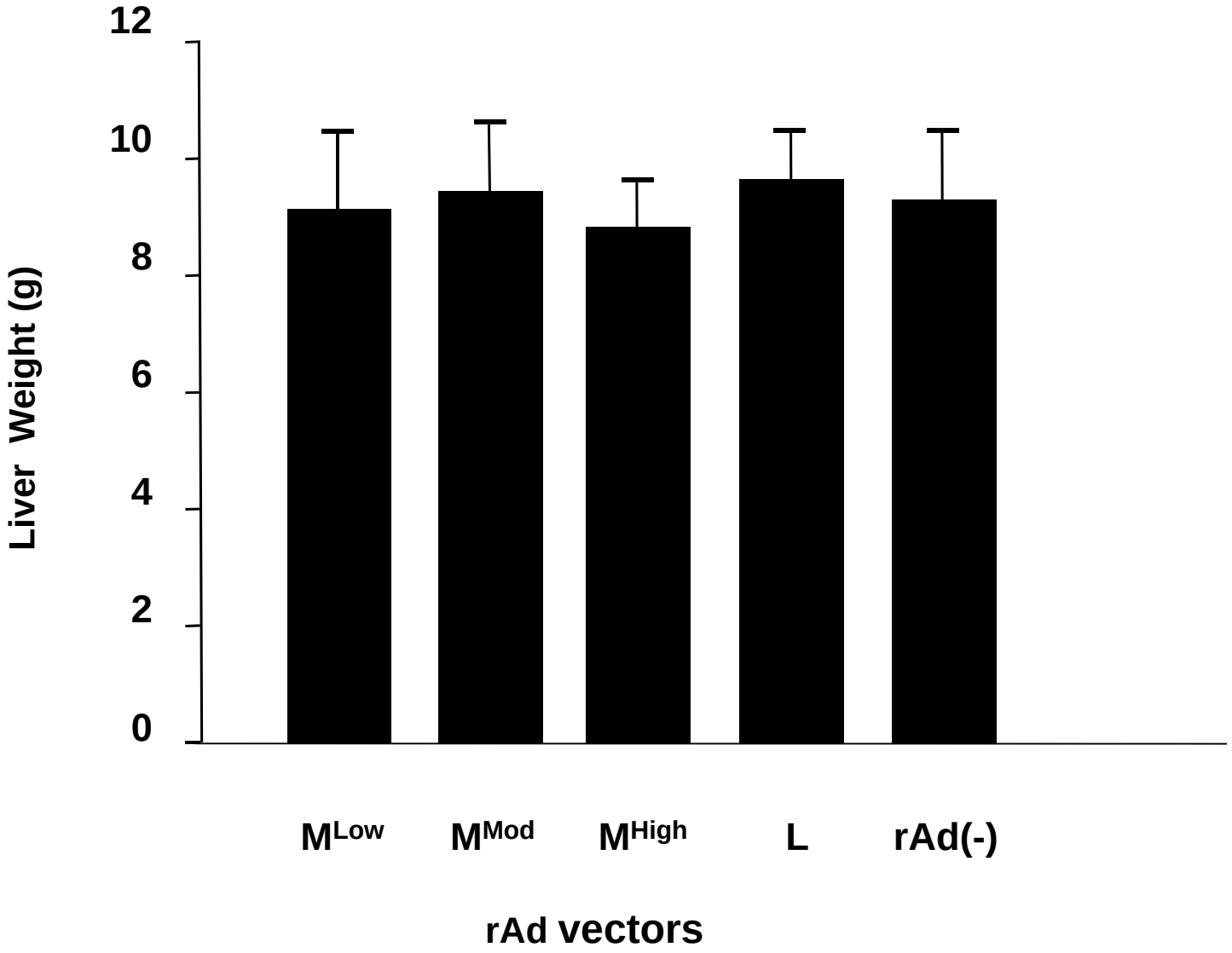

Fig 1

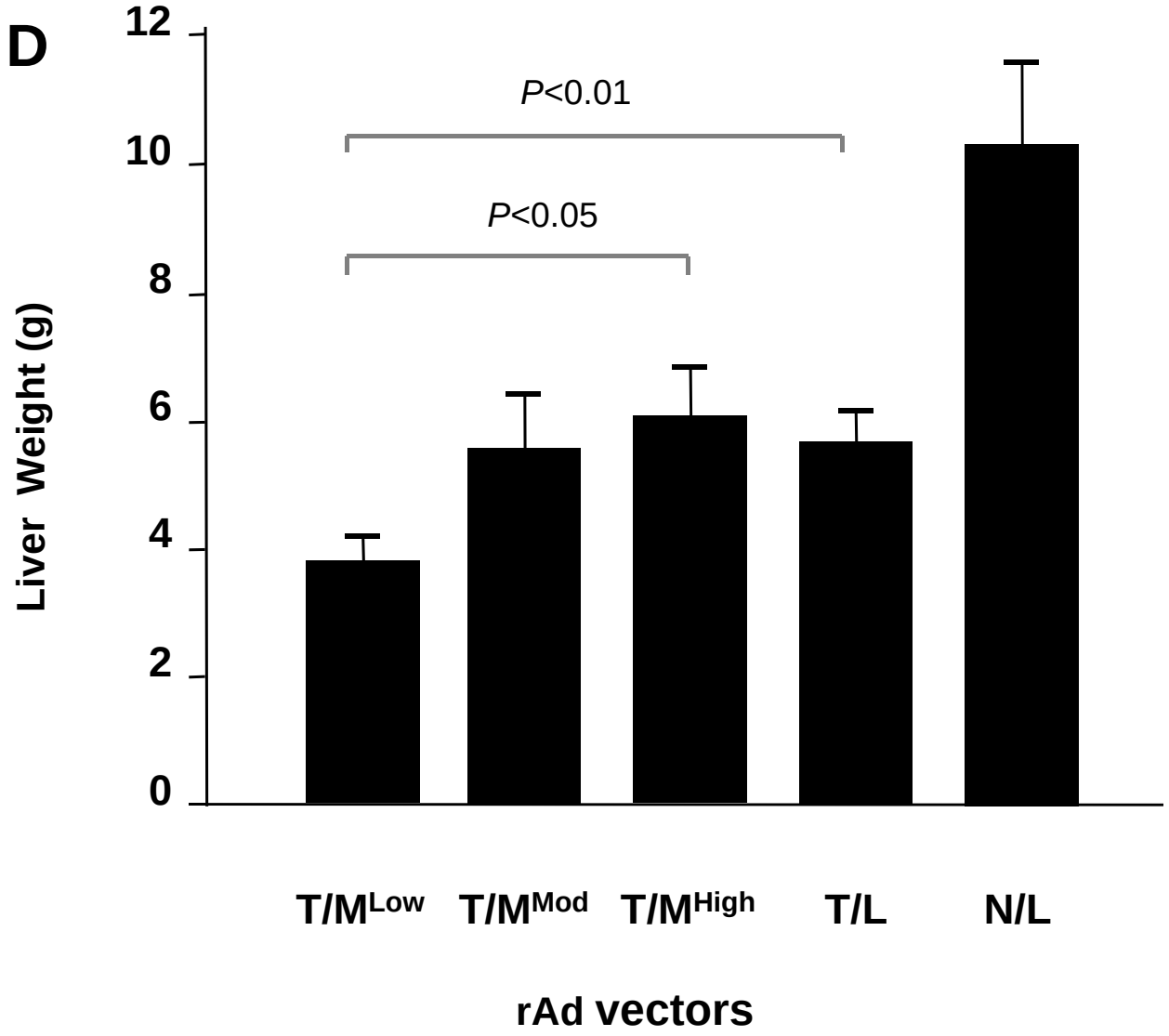
D
12
10
8
6
4
2
0
Liver Weight (g)
P<0.01
P<0.05
T/M^Low
T/M^Mod
T/M^High
T/L
N/L
rAd vectors

Fig 1

E

T/M^{low}

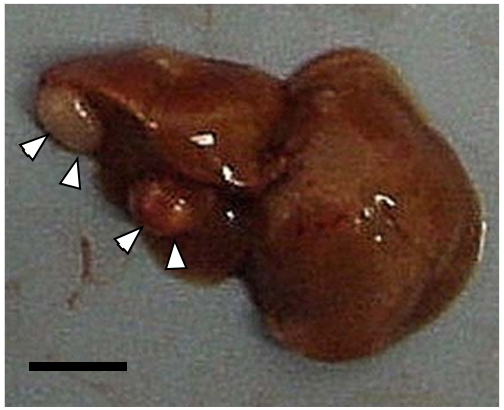

T/M^{High}

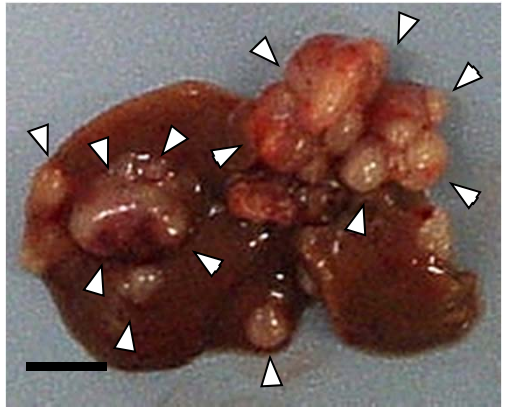

T/L

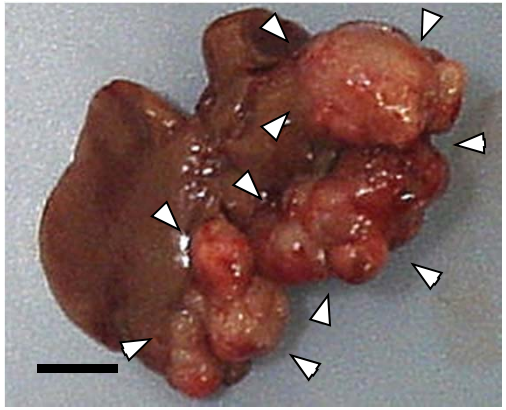

N/L

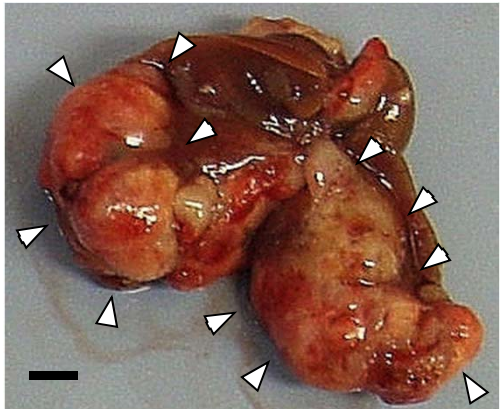

No inoculation

Fig 2

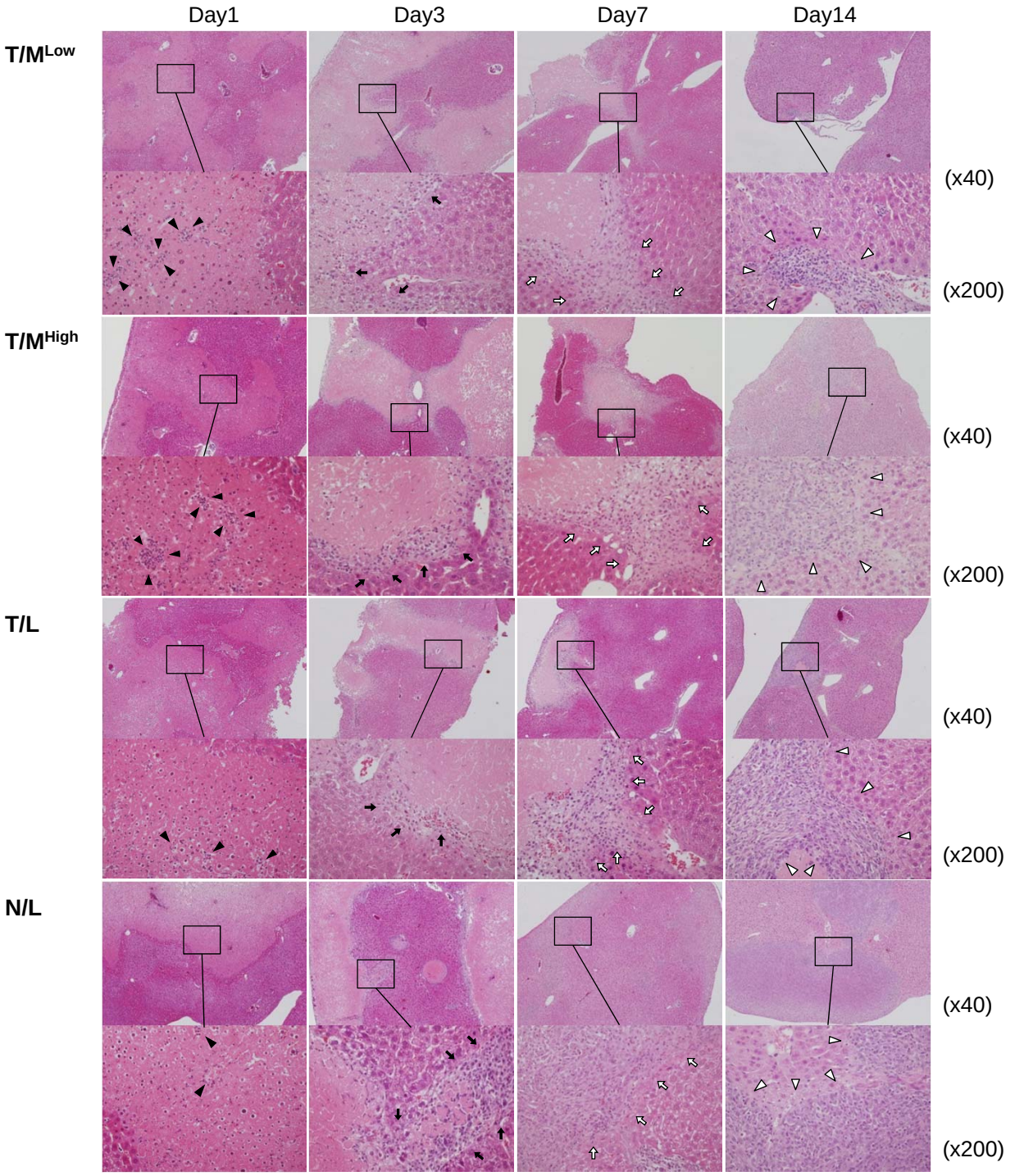
Day1
Day3
Day7
Day14
T/M^Low
T/M^High
T/L
N/L
(x40)
(x200)
(x40)
(x200)
(x40)
(x200)
(x40)
(x200)

Fig 3

A

T/M^{Low}

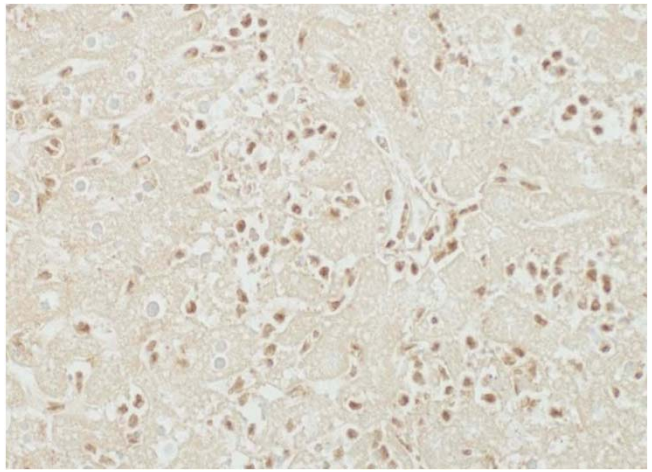

T/L

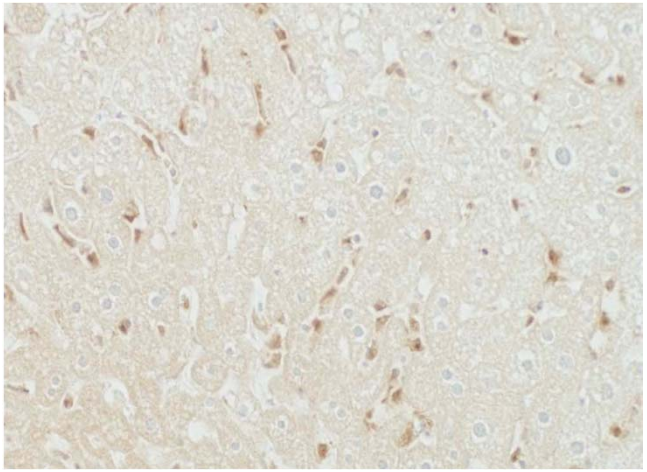

T/M^{High}

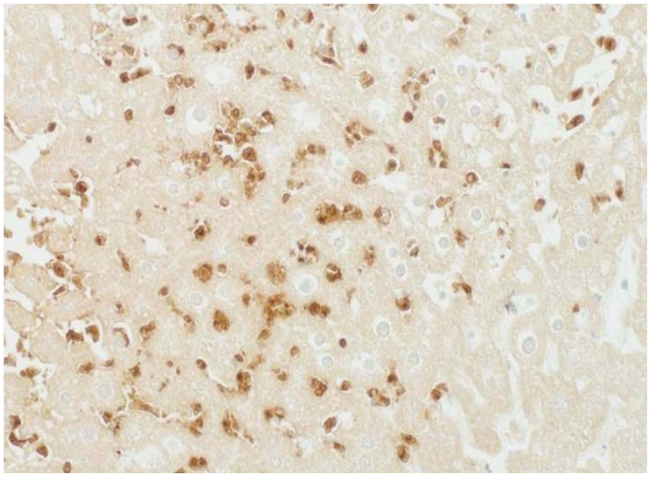

N/L

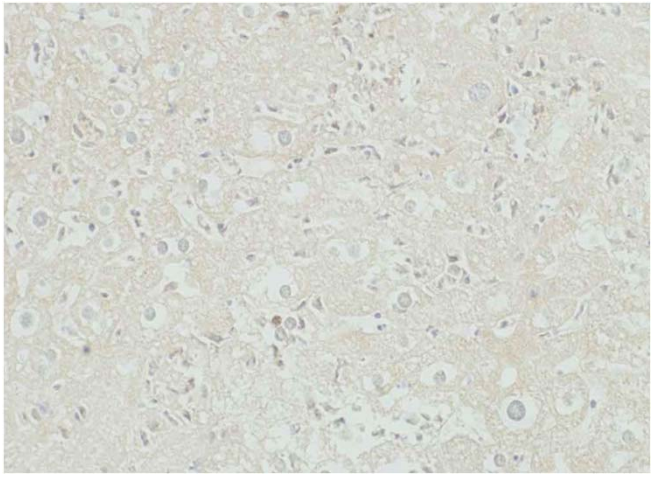

Fig 3 **B**

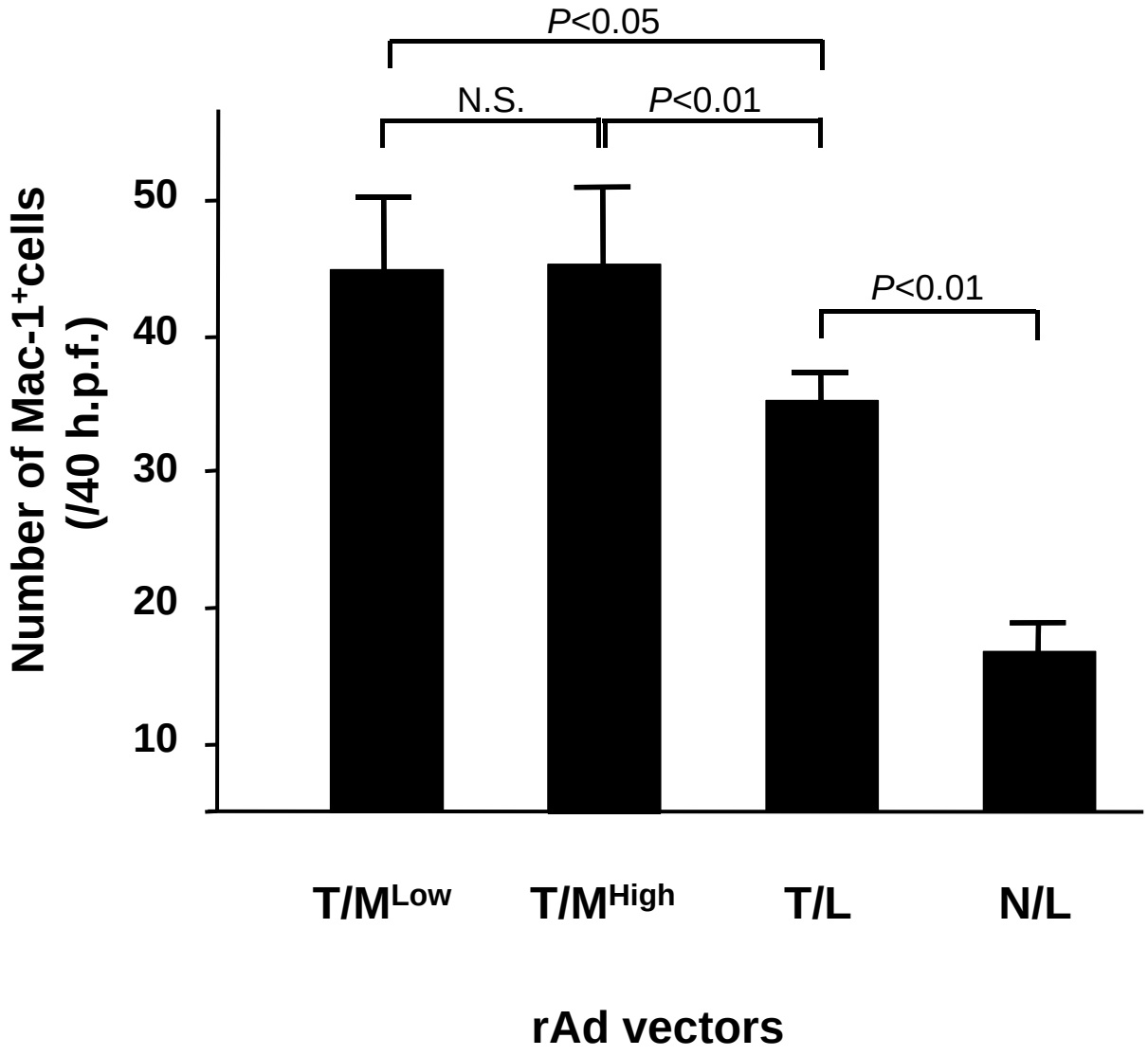
P<0.05
N.S.
P<0.01
P<0.01
Number of Mac-1+cells
(/40 h.p.f.)
50
40
30
20
10
T/MLow
T/MHigh
T/L
N/L
rAd vectors

Fig 3 C

T/M^{Low}

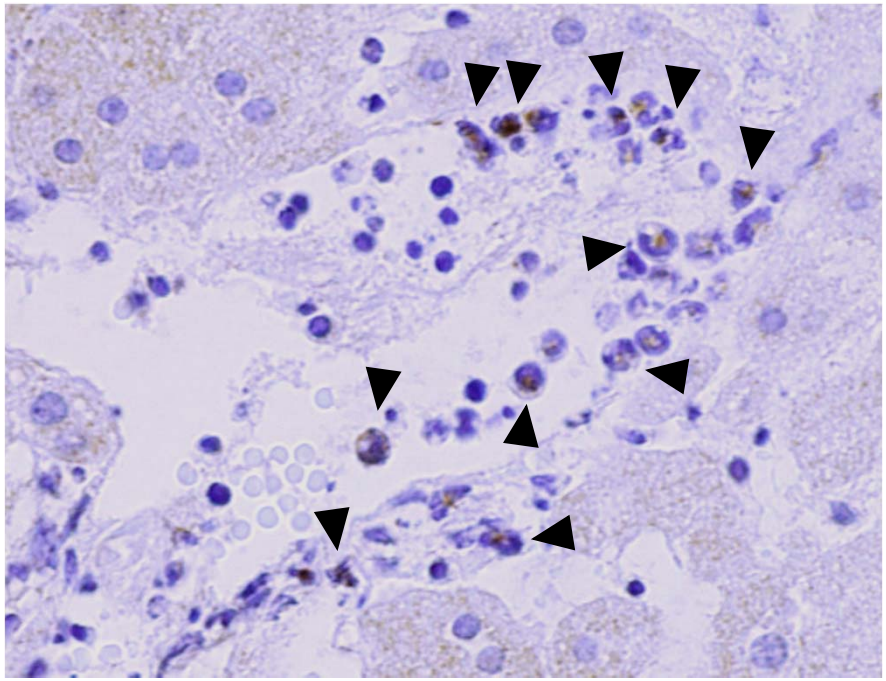

T/M^{High}

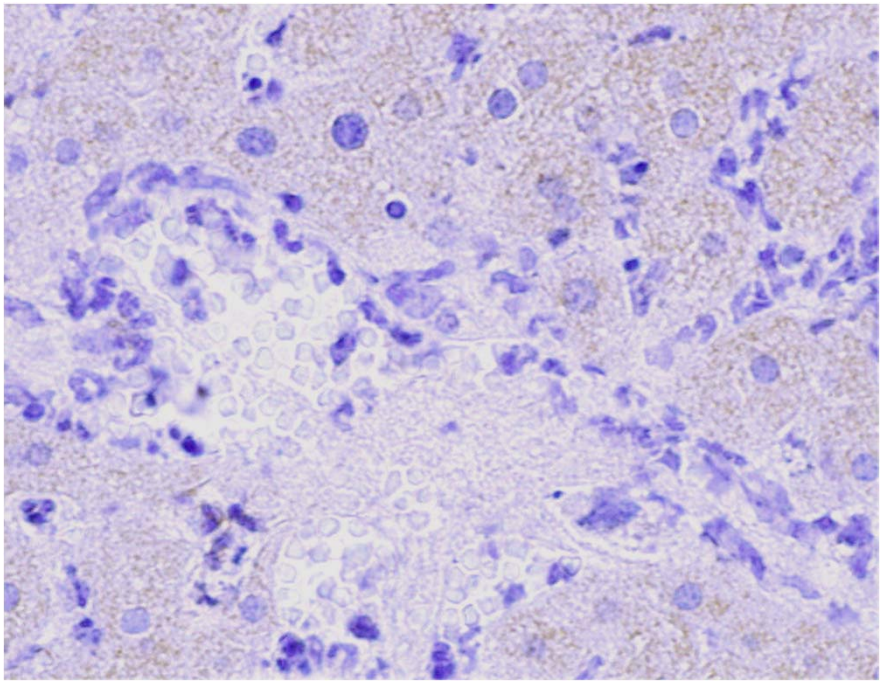

Fig 3 D

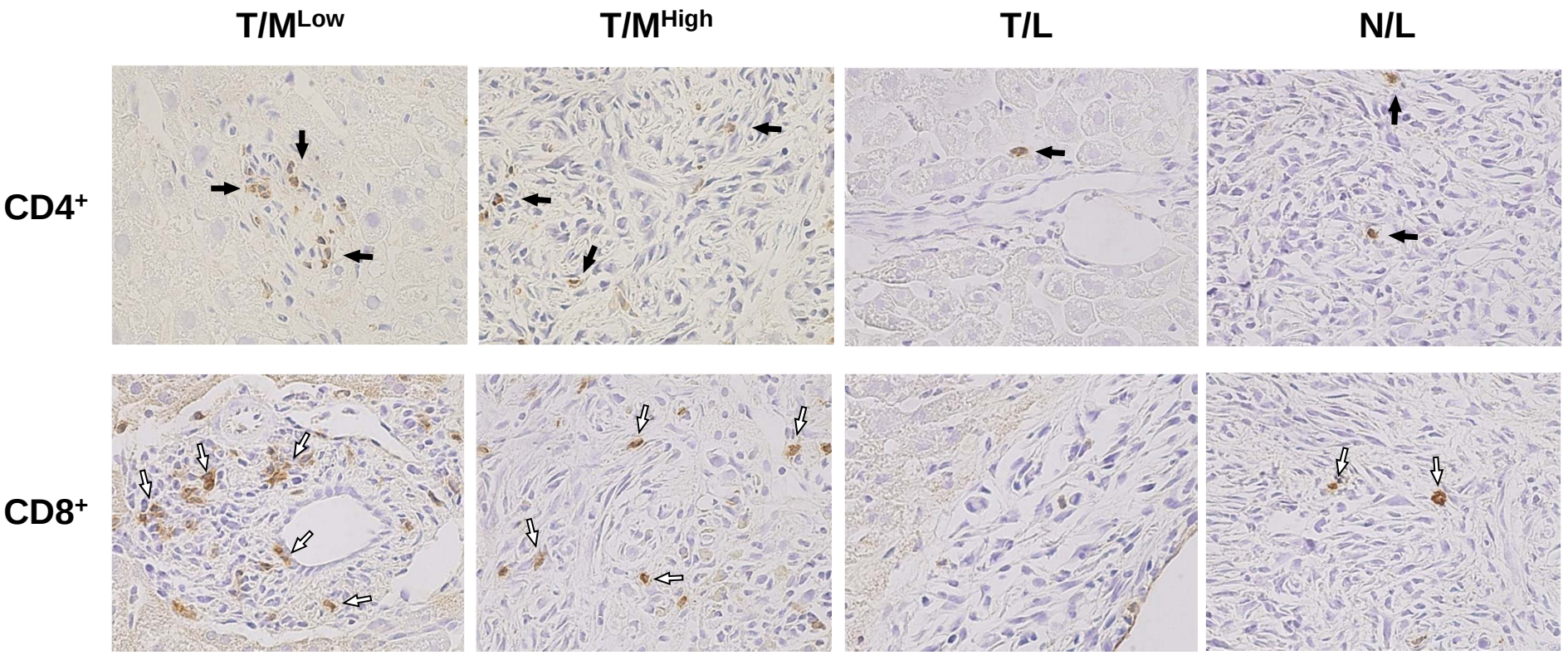

Fig 3

E

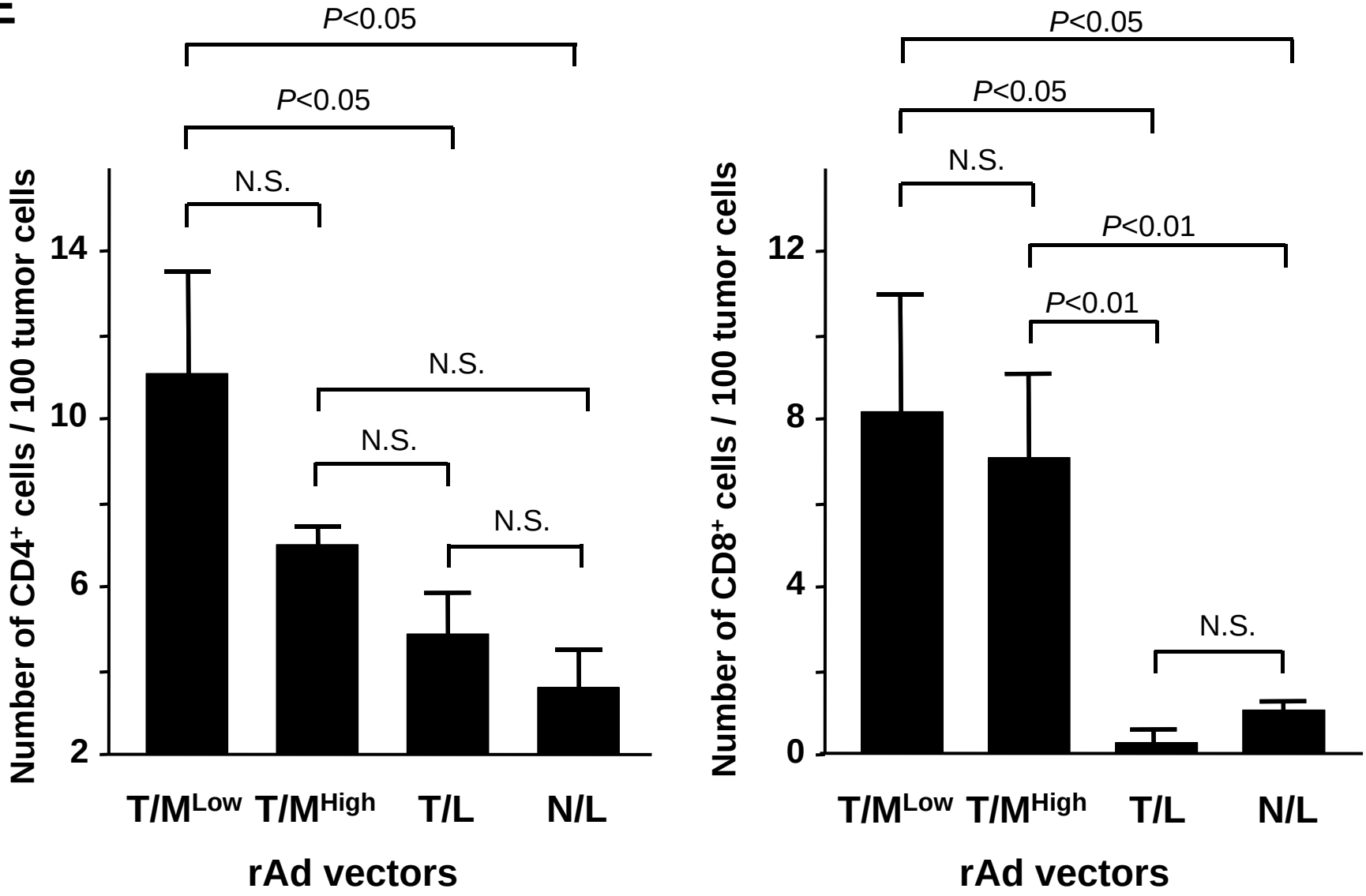
P<0.05
P<0.05
N.S.
N.S.
N.S.
N.S.
Number of CD4+ cells / 100 tumor cells
14
10
6
2
T/MLow
T/MHigh
T/L
N/L
rAd vectors
P<0.05
P<0.05
N.S.
P<0.01
P<0.01
N.S.
Number of CD8+ cells / 100 tumor cells
12
8
4
0
T/MLow
T/MHigh
T/L
N/L
rAd vectors

Fig 4

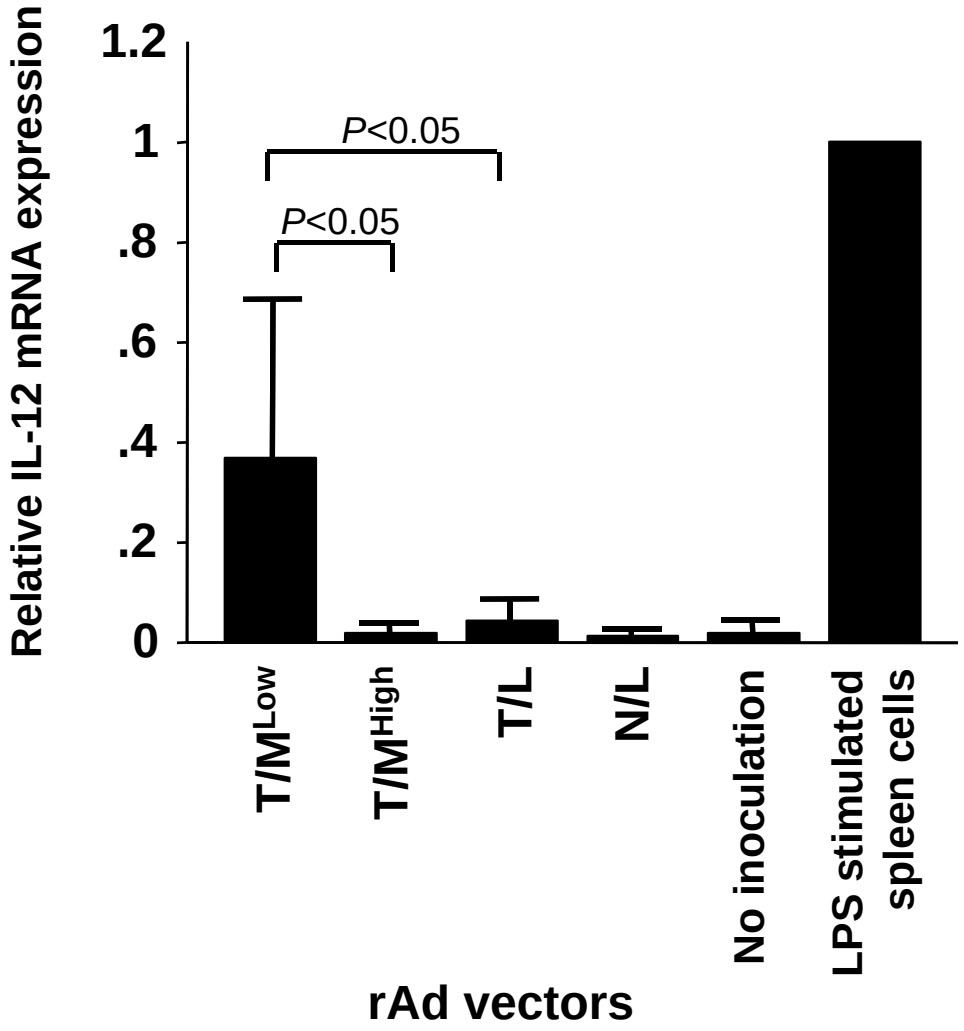
Relative IL-12 mRNA expression
1.2
1
.8
.6
.4
.2
0
P<0.05
P<0.05
T/M^Low
T/M^High
T/L
N/L
No inoculation
LPS stimulated spleen cells
rAd vectors

Fig 5 A

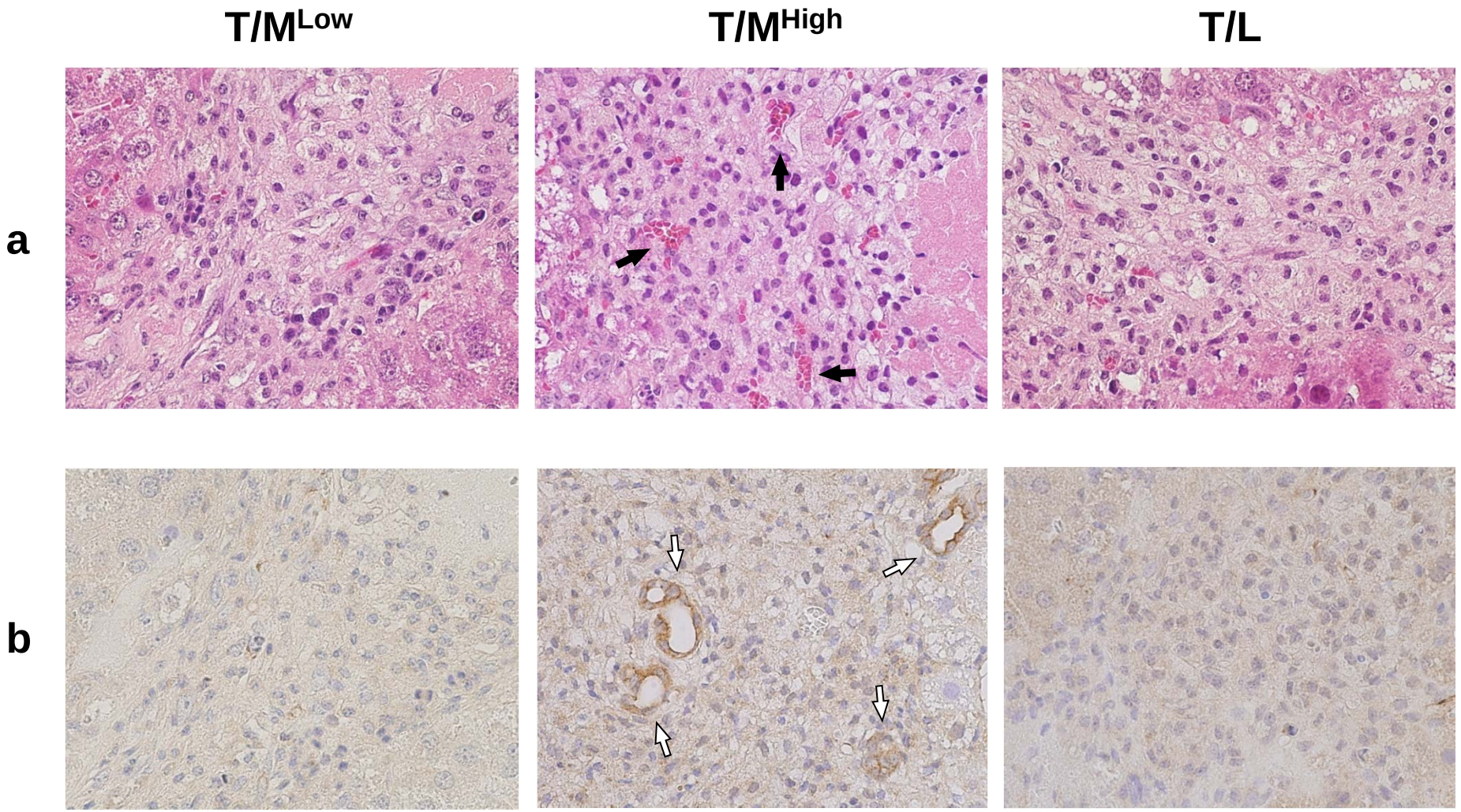

Fig 5 B

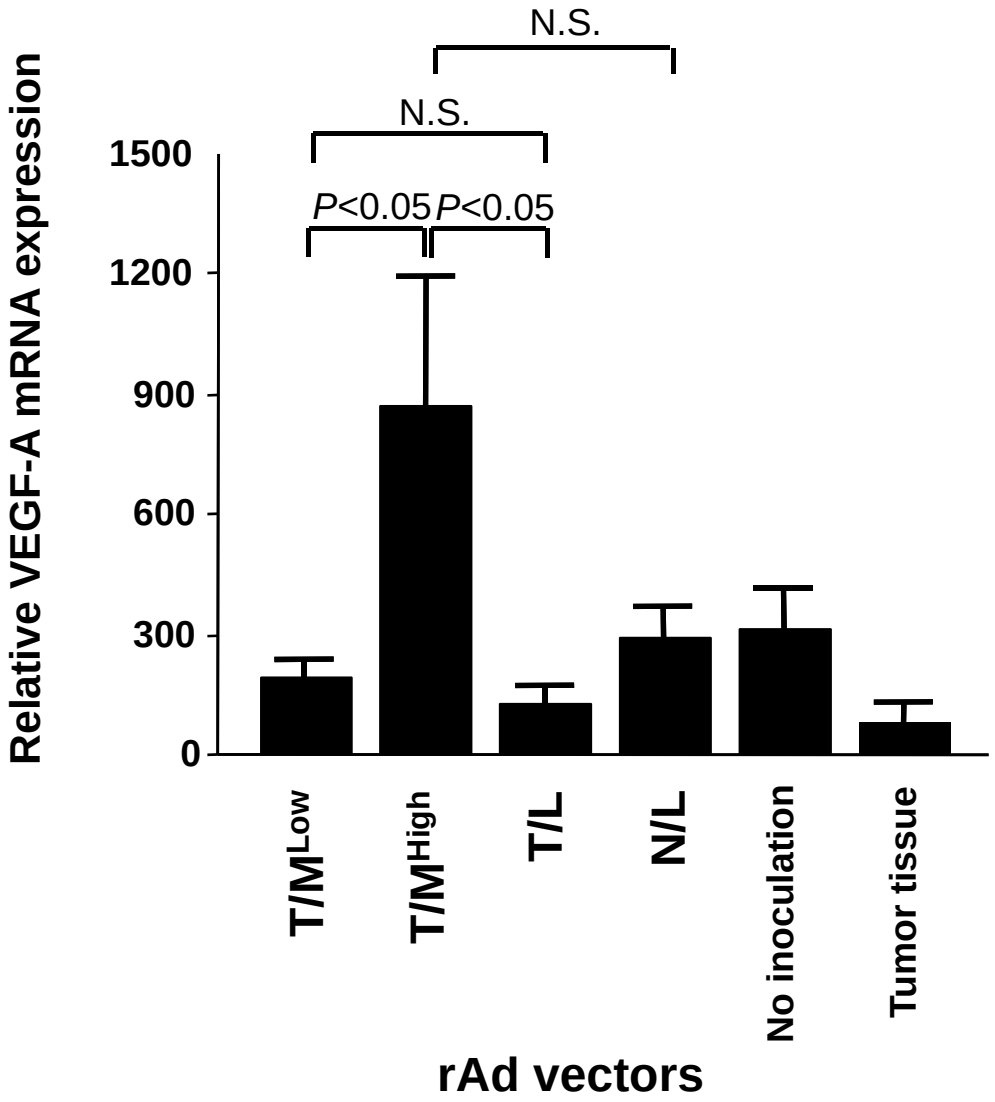
N.S.
N.S.
P<0.05
P<0.05
1500
1200
900
600
300
0
Relative VEGF-A mRNA expression
T/M^Low
T/M^High
T/L
N/L
No inoculation
Tumor tissue
rAd vectors

Fig 6

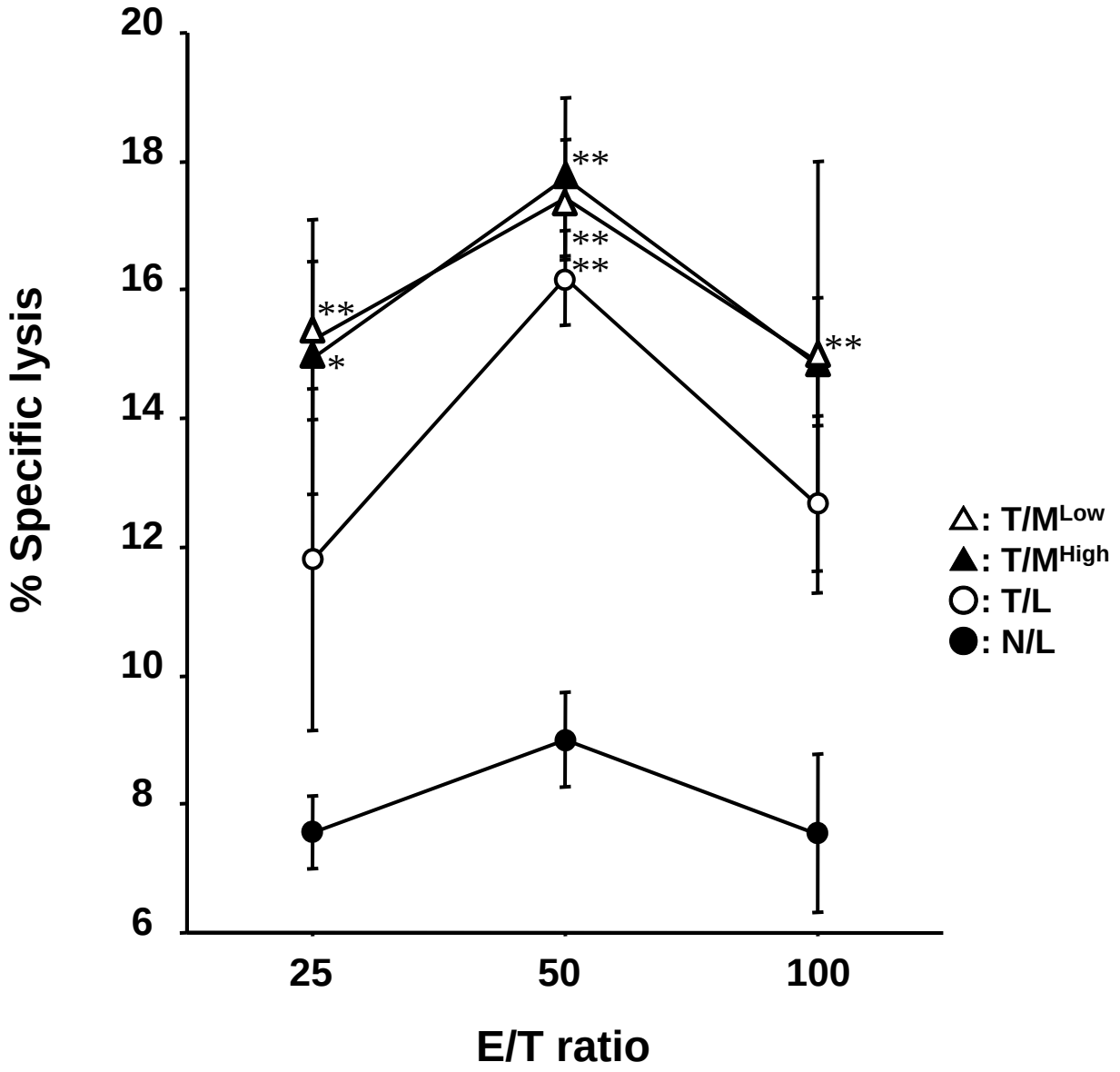
20
18
16
14
12
10
8
6
% Specific lysis
25
50
100
E/T ratio
**
**
**
*
**
△: T/M^Low
▲: T/M^High
○: T/L
●: N/L